

HD-R131 591

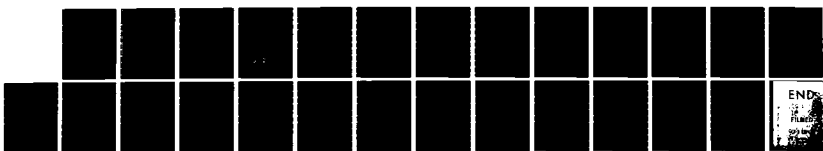
ON THE CO₂ LASER GENERATED CHANNEL CONDUCTIVITY AND
ELECTRON BEAM IONIZATION OF AMMONIA(U) NAVAL RESEARCH
LAB WASHINGTON DC A W ALI 15 AUG 83 NRL-MR-5150

1/1

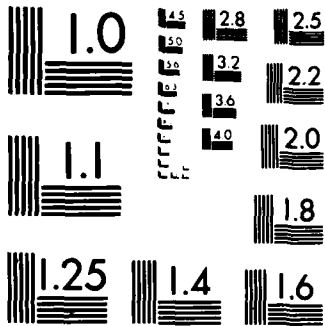
UNCLASSIFIED

F/G 20/5

NL



ENDS
111
FILMED
2018
1000



MICROCOPY RESOLUTION TEST CHART
NATIONAL BUREAU OF STANDARDS 1963-A

ADA131591

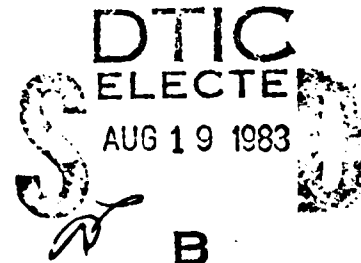
On the CO₂ Laser Generated Channel Conductivity and Electron Beam Ionization of Ammonia

A. W. ALI

Plasma Physics Division

August 15, 1983

This report was supported by Defense Advanced Research Projects Agency (DoD), ARPA Order No. 4395, Amendment 9, monitored by Naval Surface Weapons Center under Contract No. N60921-83-WR-W0088.



NAVAL RESEARCH LABORATORY
Washington, D.C.

DTIC FILE COPY

Approved for public release; distribution unlimited.

83 08 19 11 1

SECURITY CLASSIFICATION OF THIS PAGE (When Data Entered)

DD FORM 1 JAN 73 1473 EDITION OF 1 NOV 63 IS OBSOLETE
S/N 0102-014-6601

SECURITY CLASSIFICATION OF THIS PAGE (When Data Entered)

CONTENTS

I.	INTRODUCTION	1
II.	CO ₂ LASER ABSORPTION BY NH ₃	1
III.	THE NRL EXPERIMENT	2
IV.	THERMAL DISSOCIATION AND IONIZATION OF NH ₃	4
V.	THE AVALANCHE IONIZATION OF NH ₃	9
VI.	THE ELECTRON BEAM COLLISIONAL IONIZATION OF NH ₃	11
VII.	CALCULATIONS AND CONCLUSIONS	12
VII.I	THE RESIDUAL CHANNEL CONDUCTIVITY	12
VII.II	ELECTRON BEAM GENERATED CONDUCTIVITY	14
	ACKNOWLEDGMENTS	17
	REFERENCES	18

S DTIC
ELECTED
AUG 19 1983
D
B



Accession For	
NTIS GRAIL	
DATE 10/10/83	
REF ID: A6210	
CITY: STATE: ZIP:	
TYPE: DATE:	
DISTRIBUTION BY:	
Availability Codes	
Avail and/or	Special
Dist	
A	

ON THE CO₂ LASER GENERATED CHANNEL CONDUCTIVITY AND ELECTRON BEAM IONIZATION OF AMMONIA

I. INTRODUCTION

Gaseous channels with appropriate conductivity can facilitate the transport and guidance of charged particle beams and electrical discharges. Such channels can be generated by focusing a beam of high power laser or microwave radiation to breakdown the gas over the desired length. The gas breakdown results in the formation of a plasma and the heating of the gas, thereby generating a conducting channel. Studies¹⁻³ have often used CO₂ laser to form channels in various gases such as air, N₂, NH₃ and C₂H₂. The characteristics of such channels, i.e., the channel temperature and the channel conductivity must be understood in order to provide the basis for the understanding of charged particle beam transport and guidance in the channel.

In this report we present a preliminary analysis on the characteristics of NH₃ channels formed by using a CO₂ laser where the laser power is below the threshold for breakdown. The report also presents the electron beam ionization (collisional and avalanche) of NH₃ and calculates the conductivity generated by the beam for two typical experiments (NRL and Sandia Experiments). The calculation of the electron beam generated conductivity shows that the beam does its own thing in that the residual channel conductivity plays no role but a neutral density channel left behind by the laser will modify the conductivity generated by the beam. This is because the channel conductivity is either non existent or below the relevant value in these two experiments.

II. CO₂ LASER ABSORPTION BY NH₃.

The CO₂ laser is a multi-line laser, and in general it can be tuned to a given frequency. Several of the laser lines are in near resonance with absorption bands in NH₃. As an example, the v₂ mode energy diagram is shown

Manuscript approved June 14, 1983.

in Figure 1 where the CO₂ laser transitions i.e. R(16) and R(30) are shown to coincide with transitions within the v₂ band of NH₃. Such pumping in general also leads to lasing⁴ within NH₃ at frequencies smaller compared to the pump frequency. The absorption of the laser quanta by the molecule in the ground state would raise the molecule to V=1 level and several other processes of importance will occur.

1. The vibrational energy is converted to gas kinetic energy through the VT energy exchange.
2. Higher levels can be excited by further absorption of the vibrational quanta, resulting in collisionless dissociation of the molecule.
3. Vibrational-vibrational collisions resulting in the ladder type excitation and dissociation.
4. Stimulated emission.
5. Saturation of absorption.

The first process is very rapid and has a relaxation time⁵ of 2.5 nsec/atm. The second process occurs for short pulse lasers ~ in the n sec regime, while the last process occurs for lasers of long duration ~ 10 nsec.

III. THE NRL EXPERIMENT

The experiment at NRL carried out by the Channel Physics Group in the Plasma Physics Division utilizes a home made multimode CO₂ laser. This laser has⁶ a total power of (50J) and pulse length of 200 nsec. It was used to study channel physics in NH₃ where a 40 Torr NH₃ filled the chamber through which the CO₂ laser was passed in weak focus condition (The focusing was outside the chamber). The energy absorbed by the gas was 25 mJ per cm³ resulting⁷ in a temperature rise to ~ 0.1 ev.

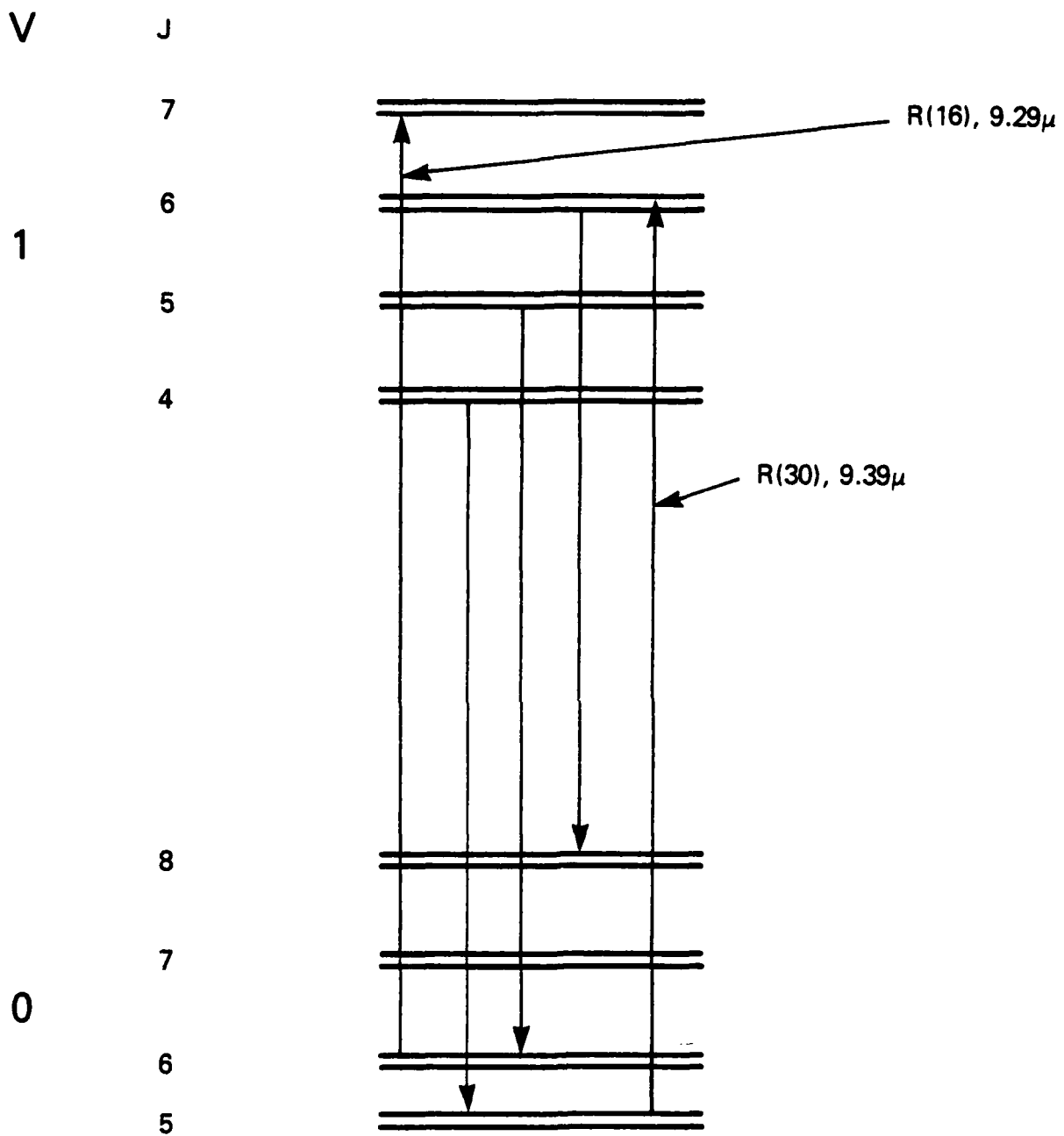


Figure 1 The v_2 mode energy diagram of NH_3 for the ground state and $V=1$ level. Two CO_2 laser bands $R(16)$ and $R(30)$ are shown to indicate the resonance absorption by NH_3 .

IV. THERMAL DISSOCIATION AND IONIZATION OF NH₃

A. In this section we will discuss the dissociation and ionization of NH₃ based on the equilibrium calculation. The absorption of CO₂ laser radiation by NH₃ and the rapid relaxation of the vibrational energy to kinetic energy justifies the equilibrium approach. This relaxation time τ_{VT} has been measured⁵ in pure NH₃ and was found to be equal to 2.5 nsec/atm. This time in the case of the NRL experiment is 47.5 nsec which is still much smaller than the pulse width (~ 200 nsec.).

The mass action law⁸ for the dissociation equilibrium is

$$\frac{H \quad NH_2}{NH_3} = K \quad (1)$$

Where K is the equilibrium constant H, NH₂ and NH₃ are the densities of the relevant species. The equilibrium constant can be expressed⁸ as

$$K = \frac{Q(H) \quad Q(NH_2)}{Q(NH_3)} e^{-\Delta E/RT} \quad (2)$$

Where Q(S) is the total partition functions of species S and is a function of temperature only. The total partition function in general is a product⁸ of translational and internal partition functions of species S i.e., $Q = Q_{\text{tv}} Q_{\text{int}}$. Thus

$$K = \left(\frac{2\pi k T M_H}{h^2} \right)^{3/2} \frac{Q_{\text{int}}(H) \quad Q_{\text{int}}(NH_2)}{Q_{\text{int}}(NH_3)} \quad (3)$$

We shall assume that the major contribution to the internal partition functions of the molecule is due to the rotational and vibrational excitation

which is always the case for poly-atomic molecules at temperatures below 1eV. The rotational partition function for NH_2 and NH_3 are⁸

$$Q_r = 0.00693 \times 10^6 \sqrt[.3]{T(I_A I_B I_C)_i} \quad (4)$$

Where I_A , I_B and I_C are the moments of inertia along the principal axis or planes. On the other hand, the vibrational partition function is⁸

$$Q_v = \pi_i \left[(1 - e^{-\omega_i hc/kT})_{\text{s}}^{d_i} \right]^{-1} \quad (5)$$

Where ω_i is the frequency of the vibrational excitation and d_i is the degree of degeneracy. Utilizing these relations into the equilibrium constant one obtains

$$K = (0.31T)^{3/2} \times 10^{21} \frac{\sqrt{(\frac{I_A I_B I_C}{\text{NH}_2)}}}{\sqrt{(\frac{I_A I_B I_C}{\text{NH}_3})}} \frac{\pi_i (1 - e^{-\omega_i hc/kT})_{\text{NH}_2}^{d_i}}{\pi_i (1 - e^{-\omega_i hc/kT})_{\text{NH}_3}^{d_i}} \exp\left(-\frac{49880}{kT}\right) \quad (6)$$

The vibrational partition function is calculated for several temperatures and are shown in Table I

TABLE I

<u>$T(^0\text{K})$</u>	<u>$Q^v(\text{NH}_2)$</u>	<u>$Q^v(\text{NH}_3)$</u>
1000	1.26	2.07
2000	1.92	5.9

The results in Table I are obtained using the following excitation energies² 0.4, 0.12, 0.43 and 0.2 for the vibrational levels of NH_3 and 0.4, 0.19 and

0.4 for NH_2 . Assuming that the moments of inertia of NH_2 and NH_3 are the same, we obtain

$$K = (0.3T)^{3/2} \times 10^{21} R(T) \exp\left(-\frac{49880}{kT}\right) \quad (7)$$

Where R is the ratio of the vibrational partition functions of NH_2 to NH_3 . If we designate α as the degree of dissociation i.e. $\alpha = \frac{H}{\text{NH}_3}$ then the mass action law can be written as

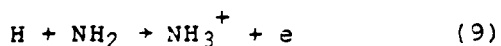
$$\alpha^2 \text{NH}_3 = K = (0.3T)^{3/2} \times 10^{21} R(T) \exp\left(-\frac{49880}{kT}\right) \quad (8)$$

Values of α for several temperatures are given in Table II for $\text{NH}_3 = 1.4 \times 10^{18} \text{ cm}^{-3}$ (~ 40 Torr).

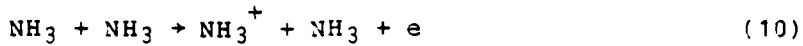
TABLE II

<u>T(°K)</u>	<u>α</u>
1160	1.2(-6)
2000	2(-2)
2200	1(-1)

B. The thermal ionization of NH_3 in most probability arises as a result of the associative ionization. i.e.



rather than



We shall calculate both rates, however, to delineate the most favorable regime.

Saha's Equation for the last process is

$$\frac{N_e}{N_{\text{NH}_3}}^2 = 2 \left(\frac{2\pi mkT}{h} \right)^{3/2} \exp(-117740/kT) \quad (11a)$$

$$\frac{N_e}{N_{\text{NH}_3}}^2 = 4.8 \times 10^{15} T^{3/2} \exp\left(-\frac{117740}{kT}\right) \quad (11b)$$

where we have assumed equal statistical weights for NH_3 and NH_3^+ . The equilibrium electron density is given in Table III for several temperatures of interest for an NH_3 density of 40 Torr.

TABLE III

<u>T(°k)</u>	<u>$N_e (\text{cm}^{-3})$</u>
1160	1.5×10^{-3}
2000	1.6×10^6
2200	2.8×10^7

Now let us consider the associative ionization process. For this we shall utilize the general cross section developed by Nelson and Dahler⁹. The threshold expression for this cross section is

$$\sigma_{ai} = \frac{2.1 R_c^2 \chi}{E} (E - E_{th})^{1.5} \quad (12)$$

Where R_c is the crossing point, E_{th} is the threshold for association and $x = 2(2\mu)^{1/2} \Gamma_c/E_d$. Here, Γ_c is the width of the transition and E_d is the derivative of the potential curve at the crossing point. Using (*) $\Gamma_c \approx 0.04$ and $R_c \approx 10^{-9} \text{ cm}^3$ i.e. $x \approx 1.6 \times 10^6$ and $E_d \approx 1.0 \times 10^{-4}$, we obtain

$$\sigma_{ai} = 4.2 \times 10^{-16} \frac{(E - 5.8)}{E}^{3/2} \quad (13)$$

where E is in units of eV. Using the slope of this cross section one obtains the following rate coefficient for the associative ionization

$$R_{ai} = 10^{-12} \sqrt{T_g} (5.8 + 2 T_g) e^{-5.8/T_g} \quad (14)$$

where T_g is in units of eV.

If we assume that the dissociative recombination rate coefficient is $10^{-6} \text{ cm}^3 \text{ sec}$, then at equilibrium we will have

$$10^{-6} N_e^2 = R_{ai} H NH_2 \quad (15)$$

Table IV gives the values of the electron density using the equilibrium values of H given in Table II

(*) Values relevant to $N + O \rightarrow NO^+ + e$

TABLE IV

<u>T(°K)</u>	<u>H (cm⁻³)</u>	<u>N_e (cm⁻³)</u>
1160	1.68 x 10 ¹²	5.8 x 10 ⁻⁴
2000	2.8 x 10 ¹⁶	2 x 10 ⁶
2200	1.4 x 10 ¹⁷	5 x 10 ⁷

If one lowers the dissociative recombination rate coefficient by an order of magnitude, the equilibrium electron density will be as in Table V.

TABLE V

<u>T(°K)</u>	<u>N_e (cm⁻³)</u>
1160	1.8 x 10 ⁻³
2000	6.3 x 10 ⁶
2200	1.5 x 10 ⁸

V. THE AVALANCHE IONIZATION OF NH₃.

The Townsend ionization coefficient for NH₃ has been measured by Risbud and Naidu¹⁰ for $\frac{E}{N}$ between $115 \times 10^{-17} \text{ v-cm}^2$ and $2060 \times 10^{-17} \text{ v-cm}^2$. The following expressions fit the data to better than 30%.

$$\frac{\alpha}{N} = 1.07 \times 10^{-14} \text{ Exp} \left(-\frac{1.23 \times 10^{-14}}{E/N} \right) \quad (16)$$

for

$$115(-17) < E/N < 182 (-17)$$

and

$$\frac{\alpha}{N} = 4.34 \times 10^{-16} \text{ Exp} \left(-\frac{65.2 \times 10^{-16}}{E/N} \right) \quad (17)$$

for

$$182(-17) < \frac{E}{N} < 2060(-17)$$

The electron drift velocity, however, is measured¹¹ over a limited range, i.e. up to $E/N = 50 \times 10^{-17}$ v-cm². We have obtained the following fit for the

$$v_d = -1.26 \times 10^6 + 2.0 \times 10^{22} (E/N) \quad (18)$$

drift velocity for the region of $\frac{E}{N}$ from 46.1×10^{-17} v-cm² to 54.2×10^{-17} v-cm². This expression can be extended to higher E/N until further data becomes available.

Using Equations 16 - 18 we obtain the following expressions for the reduced ionization frequency in NH₃

$$\frac{v_i}{N} = [-1.26 \times 10^6 + 2 \times 10^{22} (\frac{E}{N})] \times 2.0 \times 10^{-14} \text{ Exp} \left(-\frac{1.23 \times 10^{-14}}{E/N} \right) \quad (19)$$

for

$$115(-17) < E/N < 182(-17)$$

and

$$\frac{v_i}{N} = [-1.26 \times 10^6 + 2 \times 10^{22} (E/N)] 4.34 \times 10^{-16} \text{ Exp} \left(-\frac{65.2 \times 10^{-16}}{E/N} \right) \quad (20)$$

for

$$182(-17) < E/N < 2060(-17)$$

The reduced ionization frequency $\frac{v_i}{N}$ is given in Table VI.

TABLE VI

<u>E/N</u>	<u>v_i/N</u>	<u>E/N</u>	<u>v_i/N</u>
115 (-17)*	0.494 (-11)	1234 (-17)	6.17 (-8)
123 (-17)	1.14 (-11)	1543 (-17)	8.64 (-8)
154 (-17)	1.06 (-10)		
200 (-17)	6.50 (-10)		
216 (-17)	8.85 (-10)		
308 (-17)	3.08 (-9)		
462 (-17)	9.56 (-9)		
617 (-17)	1.82 (-8)		
925 (-17)	3.9 (-8)		

VI. THE ELECTRON BEAM COLLISIONAL IONIZATION OF NH₃

The electron beam ionization of NH₃ can be estimated readily, provided one knows the NH₃ stopping power for high energy electrons. For this purpose we shall assume that ammonia is neonlike and its density is equivalent to that of nitrogen atom. Using the calculated data for dE/dx for neon¹² one obtains a value of 1.96×10^3 eV/cm, in one atmosphere of NH₃, for electrons with energy of 1 MeV. This value increases by ~ 20% when the beam electron energy is 10 MeV.

(*) (-17) indicates 10^{-17}

VII. CALCULATIONS AND CONCLUSIONS

In the preceding sections we have presented the electron beam collisional and avalanche ionization parameters of NH₃. Furthermore, we presented the equilibrium calculations of an NH₃ channel generated by lasers in the temperature range of 0.1 to 0.19 eV. From these equilibrium relations we have obtained the residual electron density in the same temperature range.

In this section we would like to calculate the residual conductivity for two channels, one at a temperature of 0.1 eV (NRL Experiment) and the other at a temperature of 0.19 eV (Sandia Experiment). Then we will calculate the conductivity generated by two electron beams, one with a radius of 1 cm, a peak current of 8 kA and a current rise time of 20 nsec (NRL Experiment) and the other with a radius of 1 cm, a peak current of 50 kA and a current rise time of 60 nsec (Sandia Experiment). These calculations can be made readily for a short time (1 nsec), which is sufficient enough to provide the needed information on the conductivity generated by the beam.

VII.I THE RESIDUAL CHANNEL CONDUCTIVITY

The conductivity of the channel can be expressed by

$$\sigma = 2.5 \times 10^8 N_e / v_m \quad (21)$$

where v_m is the momentum transfer collision frequency of electrons in NH₃. The cross section for the electron momentum transfer in NH₃ has been measured by Pack, et al¹¹ and is shown in Figure 2. In this figure, the electron momentum transfer cross section¹³ in N₂ is also shown for comparison.

The momentum transfer collision frequencies in 40 Torr of NH₃ with electron temperatures of 0.1 and 0.2 eV are $\sim 2.7 \times 10^{11} \text{ sec}^{-1}$ and 4×10^{11}

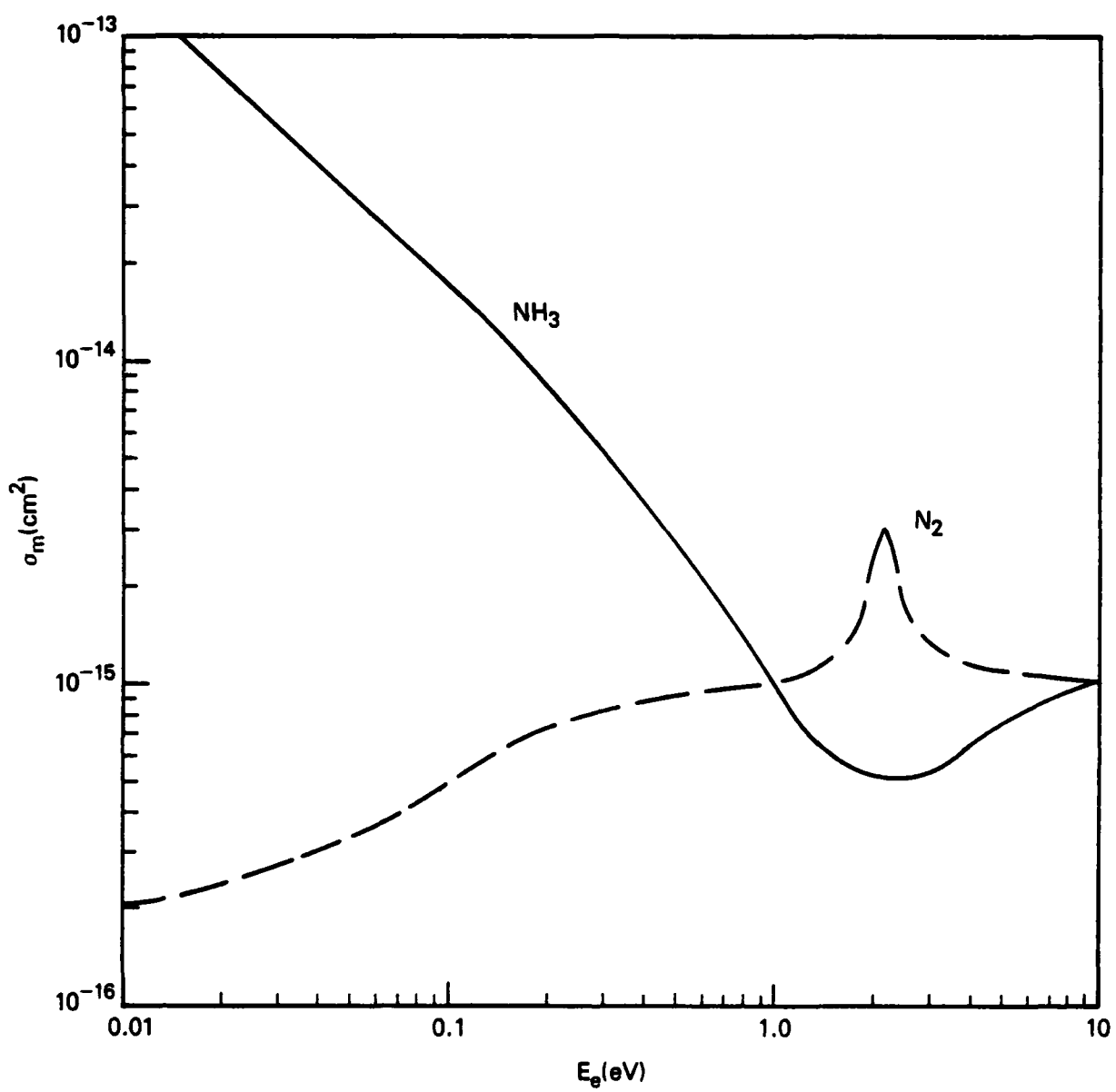


Figure 2 The electron momentum transfer cross section in ammonia and N₂.

sec^{-1} , respectively, corresponding to the experiments of NRL and Sandia. Thus the residual conductivities in these experiments are 10^{-6} sec^{-1} (NRL) and 10^{+5} sec^{-1} (Sandia). The non-existence of conductivity at the NRL experiment has been borne⁷ out by the measurements at NRL. It should be noted (See Figure 2) that when the plasma electron energy increases (when the electron beam enters the channel) the momentum transfer cross section becomes smaller and hence would the collision frequency. The product of σv varies from 3.4×10^{-7} to 6×10^{-8} for electron energy of 0.1 eV to 1.0 eV which implies a lowering of v_m by a factor of ~ 6 . Even if this factor could become an order of magnitude the residual conductivity in the Sandia experiment would still be $\sim 10^6 \text{ sec}^{-1}$, which is much below 10^9 sec^{-1} .

VII.II ELECTRON BEAM GENERATED CONDUCTIVITY

A simple hand calculation for the beam ionization in ammonia for the NRL and Sandia Experiments is shown in Figure 3 indicating that the beam generates much more electrons, and in a short time, compared to the residual electron density. These calculations are based on the assumption that E_z is constant for times shorter than 1 nsec. and that $I_n = I_b$. With this the electric field for the Sandia Experiment is twice that of NRL.

In Figure 4 we show the electron production rates for direct and avalanche processes in both NRL and Sandia Experiments, based on a more sophisticated model¹⁴. This model solves the rate equations for ionization coupled to a simple circuit equation for E_z . These results show that the role of avalanche ionization is more discernible in the Sandia Experiment than that of NRL. Also if the channel is assumed to be rarefied (due to heating) by a factor of 6, the avalanche ionization in Sandia Experiment plays an important role compared to the direct beam ionization.

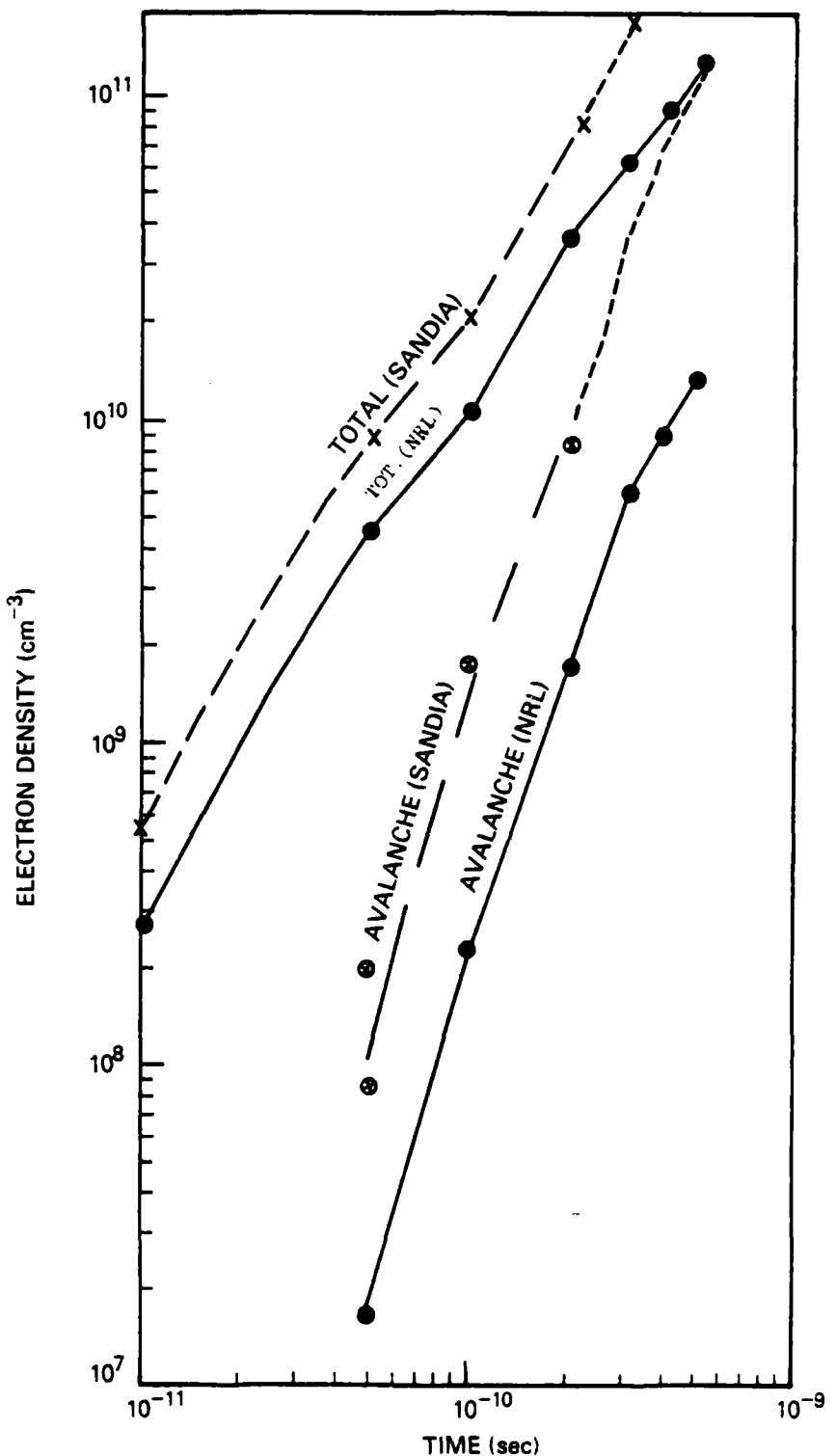


Figure 3 The electron density build up in 40 Torr of ammonia due to beam interaction. The avalanche contribution is shown separately for two experiments (NRL and Sandia).

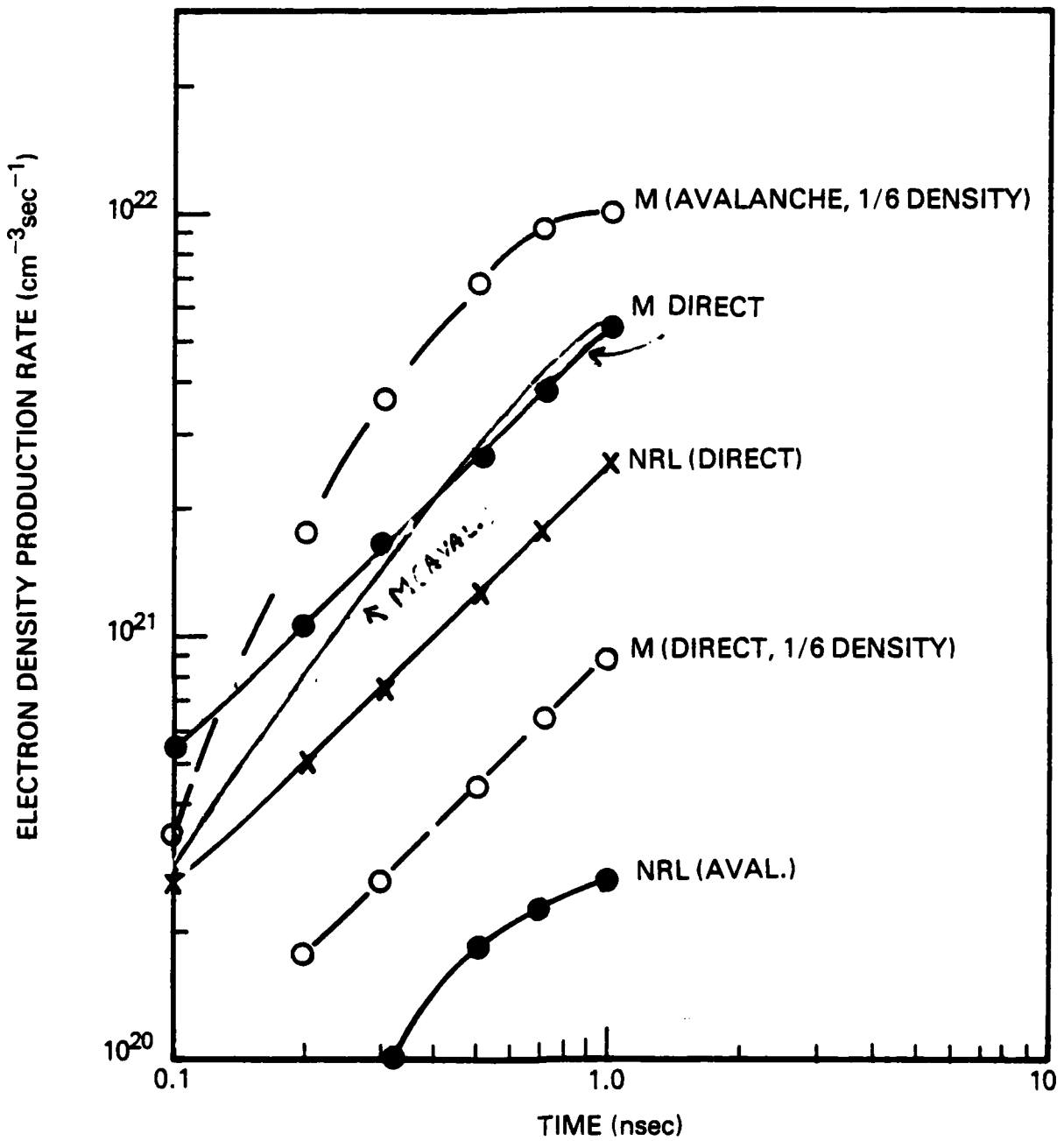


Figure 4 The electron density production rate in 40 Torr of ammonia. Direct beam collisional ionization and avalanche contributions are indicated. The density reduction by a factor of 6 is also shown for the Sandia Experiment.

In conclusion one could say that in both experiments the beam does its own thing and that the small or non existent residual conductivity in the laser heated channel adds very little to the beam generated conductivity. However, the neutral density channel left behind by the laser will modify the conductivity generated by the beam.

Acknowledgments: I wish to thank Drs. Greig and Murphy of NRL for discussion of the channel experiment in ammonia, Dr. Slinker (JAYCOR) for programing the relevant rate equations and providing me with Figure 4 and Dr. Lampe for some editorial comments.

REFERENCES

1. J. R. Greig, D. W. Koopman, R. F. Fernsler, R. E. Pechacek, I. M. Vitkovitsky and A. W. Ali, Phys. Rev. Lett. 41, 174 (1978) and references therein.
2. J. N. Olsen, J. Appl. Phys. 52, 3279 (1981).
3. J. N. Olsen and L. Baker, J. Appl. Phys. 52, 3286 (1981).
4. B. J. Vasilev, A. Z. Grasyuk, A. P. Dyadkin, A. N. Sukhanov and A. B. Yastrebkov, Sov. J. Quant. Electr. 10, 64 (1980).
5. H. E. Bass and T. G. Winter, J. Chem. Phys. 56, 3619 (1972).
6. J. R. Greig, Naval Research Laboratory "Private Communication" 1982.
7. D. Murphy, Naval Research Laboratory "Private Communication" 1982.
8. G. Herzberger, "Molecular Spectra and Molecular Structure" I - Spectra of Diatomic Molecules, Van Nostrand, New York (1950).
9. S. E. Nielson and J. S. Dahler, J. Chem. Phys. 71, 1910 (1979).
10. A. V. Risbud and M. S. Naidu, J. Phys. (Paris) Colloq. C7 40, 77 (1979).
11. J. L. Pack, R. E. Voshall and A. V. Phelps, Phys. Rev. 127, 2084 (1962).
12. L. Pages, E. Bertel, H. Joffre and L. Sklavenitis, Atomic Data 4, 1 (1972).
13. A. G. Englehardt, A. V. Phelps and G. G. Risk, Phys. Rev. 135. A 1566 (1964).
14. A. W. Ali and S. Slinker (to be published).

DISTRIBUTION LIST

Chief of Naval Operations
(Attn: Dr. C. F. Sharn (OP0987B))
Washington, D.C. 20350

Air Force Weapons Laboratory
Kirtland Air Force Base
Albuquerque, New Mexico 87117

ATTN: Dr. K. Dreyer
Dr. D. Straw
Dr. R. Lemke
Dr. C. Clark

U.S. Army Ballistics Research Laboratory
Aberdeen Proving Ground, Maryland 21005
ATTN: Dr. D. Eccleshall (DRXBR-BM)

Ballistic Missile Defense Advanced Technology Center
P.O. Box 1500
Huntsville, Alabama 35807
ATTN: Dr. M. Hawie (BMDSATC-1)

Lawrence Livermore Laboratory
University of California
Livermore, California 94550
ATTN: Dr. R. J. Briggs
Dr. T. Fessenden
Dr. E. P. Lee
Dr. S. Yu
Dr. J. Boyd

Mission Research Corporation
735 State Street
Santa Barbara, California 93102
ATTN: Dr. C. Longmire
Dr. N. Carron
Dr. M. Schiebe

National Bureau of Standards
Gaithersburg, Maryland 20760
ATTN: Dr. Mark Wilson

Commander
Naval Sea Systems Command
Dept. of the Navy
Washington, D. C. 20362
ATTN: Dr. D. Finkleman, PMS405

Science Applications, Inc.
Security Office
5 Palo Alto Square, Suite 200
Palo Alto, California 94304
ATTN: Dr. R. R. Johnston
Dr. Leon Feinstein
Dr. D. Keeley

JILA
University of Colorado
Boulder, CO 80309
ATTN: Dr. Arthur Phelps

Naval Surface Weapons Center
White Oak Laboratory
Silver Spring, Maryland 20910
ATTN: Mr. R. J. Biegalski
Dr. C. M. Huddleston
Dr. M. H. Cha, R41
Dr. H. S. Uhm, R41
Dr. R. B. Fiorito, R41
Dr. R. Cawley
Dr. Hsing-Cheng R. Chen

C. S. Draper Laboratories
Cambridge, Massachusetts 02139
ATTN: Dr. E. Olsson
Dr. L. Matson

Physical Dynamics, Inc.
P. O. Box 1883
La Jolla, California 92038
ATTN: Dr. K. Brueckner

Office of Naval Research
Department of the Navy
Arlington, Virginia 22217
ATTN: Dr. W. J. Condell (Code 421)
Dr. T. Berlincourt (Code 464)
Dr. C. Roberson

Avco Everett Research Laboratory
2385 Revere Beach Pkwy.
Everett, Massachusetts 02149
ATTN: Dr. R. Patrick
Dr. Dennis Reilly

Defense Technical Information Center
Cameron Station
5010 Duke Street
Alexandria, VA 22314 (2 copies)

Office of Naval Technology
800 North Quincy Street
Arlington, VA 22217
ATTN: Dr. E. Zimet, MAT-0712

Naval Research Laboratory
Washington, D.C. 20375
ATTN: M. Lampe - Code 4792
J. R. Greig - Code 4763
T. Coffey - Code 4000
S. Ossakow - Code 4700 (26 copies)
Library - Code 2628 (20 copies)
A. W. Ali - Code 4700.1 (30 copies)
B. Hui - Code 4790
M. Picone - 4040
J. Boris - 4040
J. B. Aviles - 6650

Defense Advanced Research Projects Agency
1400 Wilson Blvd.
Arlington, Virginia 22209
ATTN: Dr. J. Mangano
Lt. Col. R. Gullickson

JAYCOR
205 S. Whiting St.
Alexandria, Virginia 22304
ATTN: Drs. D. Tidman
R. Hubbard
S. Slinker

Mission Research Corp.
1720 Randolph Road, S.E.
Albuquerque, NM 87106
ATTN: Dr. Brendan Godfrey
Dr. L. Wright

Pulse Sciences, Inc.
1615 Broadway, Suite 610
Oakland, CA 94612
ATTN: Dr. S. Putnam

McDonnell Douglas Research Laboratories
Dept. 223, Bldg. 33, Level 45
Box 516
St. Louis, MO 63166
ATTN: Dr. Michael Greenspan
Dr. C. Leader

Sandia Laboratories
Albuquerque, NM 87185
ATTN: Dr. Bruce Miller
Dr. Barbara Epstein
Dr. John Olsen
Dr. Don Cook

Beers Associates, Inc.
P. O. Box 2549
Reston, VA 22090
ATTN: Dr. Douglas Strickland

R and D Associates
P.O. Box 9695
Marina del Rey, California 90291
ATTN: Dr. F. Gilmore

Director
Defense Nuclear Agency
Washington, D.C. 20305
ATTN: Dr. C. Fitz (RAAE)
Dr. P. Lunn (RAAE)
Mr. G. Baker

Los Alamos National Laboratory
Mail Station 5000
P. O. Box 1663
Los Alamos, NM 87545
(Attn: Dr. H. O. Dogliani
Dr. Thomas P. Starke
Dr. M. Buchwald
Dr. D. Sappenfield

Prof. David Hammer
Laboratory of Plasma Studies
Room 290
Grumman Hall
Cornell University
Ithaca, NY 14853

